

Reduced-order models of stress-stiffened MEMS structures

*Mathew Varghese, **Vladimir L. Rabinovich and *Stephen D. Senturia

*Massachusetts Institute of Technology, Cambridge, MA, USA, varghese@mtl.mit.edu, sds@mtl.mit.edu

**Microcosm Technologies Inc., Cambridge, MA, USA, rv1@memcad.com

ABSTRACT

We present a process for generating reduced-order models for stress-stiffened MEMS structures. The models are created using the established CHURN process, which uses non-linear, analytic, energy functions to describe the state of each conservative quasi-static energy domain (electrostatic, magnetostatic, elastostatic) in the MEMS structure. Equations of motion for the structure are constructed from the energy functions using Lagrangian mechanics. Our new contribution is the generation of an accurate analytic function that captures the non-linear elastic potential energy (strain energy) of the structure.

Keywords: macromodels, energy methods, MEMS, stress-stiffening, modal-methods

1 INTRODUCTION

Electrostatically actuated MEMS devices involve the tight coupling between the mechanical and electrostatic energy domains. 3-D meshed simulation, involving the solution of thousands of equations, is effective at modeling static actuation of these devices, however, modeling dynamics is computationally challenging and very slow. For this reason, dynamic system level simulations of devices and their associated electronics is impractical. To perform these simulations it is useful to have relatively small and fast models that capture the essential physics of the device in a form that is easily inserted into system level simulators such as SPICE, or SABER. These models are typically called “reduced-order” models or “macromodels.”

Gabbay et al. [1] demonstrated an automated method of generating such models where a small set of linear elastic modes form basis functions that describe the position of the MEMS structures. The construction of these models is referred to as the CHURN process. Ultimately, the representation of the device is a set of equations describing motion and expressed in terms of the basis function amplitudes.

$$m_i \frac{d^2 q_i}{dt^2} = F_{m,i}(\bar{q}, t) + F_{e,i}(\bar{q}, t) = -\frac{\partial U_m(\bar{q})}{\partial q_i} + \frac{\partial U_e^*(\bar{q})}{\partial q_i} \quad (1)$$

where m_i is the generalized modal mass, q_i is the modal (basis function) amplitude, $F_{m,i}$ and $F_{e,i}$ are the mechanical and electrostatic forces acting on the mode, U_m is the elastic potential energy and U_e^* is the electrostatic co-energy.

The CHURN process computes analytical expressions, in terms of basis function amplitudes, of the energies U_m and U_e^* from data sets of mechanical simulations and electrostatic simulations, respectively. Fully coupled meshed electromechanical simulations are avoided.

The success of this energy based method is very much dependent on the choice of basis functions representing the position or deformation of the device. Gabbay found that using just a few low order modes of typical MEMS devices was sufficient to describe problems involving non-linear electrostatics and linear mechanics. However, when deflections of structures were on the same order as their thickness, the models failed to represent the mechanical stiffness correctly. Under such deflections the real device undergoes Poisson contraction and axial stretching in a process referred to as stress stiffening. This involves the excitation of very high order modes that are *not* included in the CHURN model. The model constrains motion to low order modes and does not allow relaxation in the higher order modes that represent the effects of stress stiffening. The positional change associated with the relaxation is very small relative to the low order modes, but not including it significantly affects the elastic strain energy. Given this, one solution might be to include all the high order modes necessary to represent relaxation. However, attempting to include more modes in the CHURN formulation is undesired for several reasons -- the order of the model increases, the construction of the model becomes more time consuming and difficult, and the determination of the relevant high order modes is impractical. Mehner et al. [2] demonstrated that if the original modal basis functions were modified slightly, one could calculate a mechanical strain energy function that reflected the effects of stress-stiffening without having to include more modes. Their approach, however, only applies to a useful, but restricted, class of structures. We present a more general approach to solving this problem that is amenable to automation.

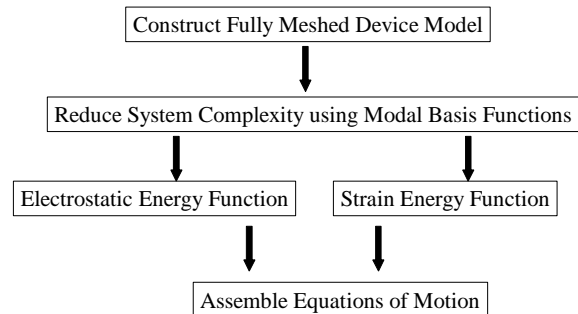


Figure 1: Overview of macromodel construction.

2 THEORY

An overview of the construction of a macromodel is shown in *Figure 1*. It is identical to the CHURN process, except for the method of generating the strain energy function.

We begin with a fully meshed model of our device, and from this generate the first few linear elastic modes. These are the eigenvectors of the equation:

$$[M]\ddot{\bar{y}} + [K]\bar{y} = 0 \quad (2)$$

M is the mass matrix, K is the stiffness matrix, and y is a vector representing the positional state of nodes in the meshed device. We then make the assumption that a well chosen set of m modes can represent the practical deformations of our device accurately according to:

$$\bar{y} = \bar{y}_{eqm} + \sum_i^{All} q_i \bar{\mathbf{j}}_i \approx \bar{y}_{eqm} + \sum_i^m q_i \bar{\mathbf{j}}_i = \mathbf{y}_0(q_1, \dots, q_m) \quad (3)$$

where y_{eqm} is the equilibrium positional state of the system, \mathbf{j}_i is the mode shape, q_i is the mode amplitude, and m is the number of modes we choose to use. \mathbf{y}_0 represents the configuration function that takes the generalized coordinates q_1, \dots, q_m and determines the positional state of the mesh.

The CHURN process takes superpositions of modes according to (3) and computes the associated electrostatic co-energy using a meshed simulation. A polynomial, U_e^* , is then fit to a data set obtained by repeating this procedure for many different mode amplitudes.

$$U_e^*(q) = \sum_{i=0}^{R_1} \dots \sum_{i_m=0}^{R_m} a_{i_1 \dots i_m} q_1^{i_1} \dots q_m^{i_m} \quad (4)$$

R_m is the maximum order of basis function m , and a_i are the fitting parameters. The user is required to specify R_m , after which the fitting is done automatically. In order to reduce the number of terms in the polynomials, we included only terms of the form, $q_m^{i_m}$, $q_i q_j$ and $q_i q_j^2$. This reduces the total number of terms in the polynomial significantly while retaining a good fit.

Figure 2 shows how the CHURN process is modified to calculate the strain energy function. Once the modes are chosen, we calculate the linear reaction forces at each mesh node, f_i , associated with displacing the structure into each mode shape. We then apply a superposition of these modal forces as a load on the device and calculate the resulting displacement and strain energy. For linear mechanics, the modal component amplitude q_i of the resulting structure, is exactly the same as the amplitude of the applied modal forces, p_i .

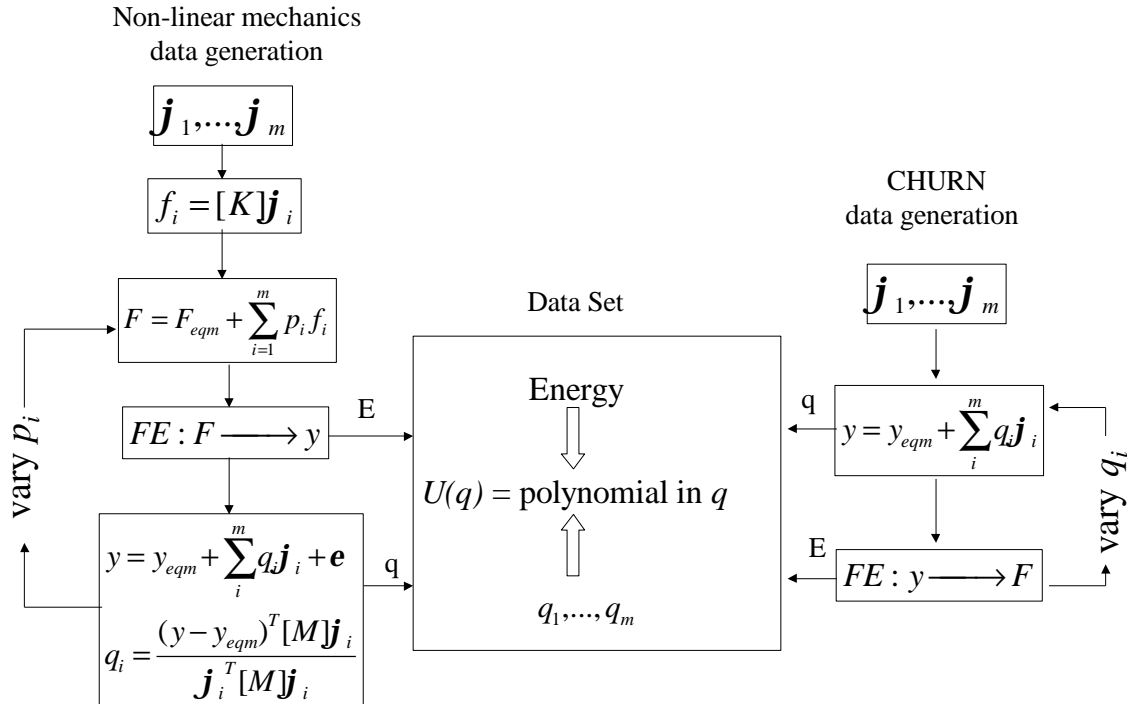


Figure 2: Overview of the data generation for the non-linear mechanics and CHURN processes. \mathbf{j}_i is a vector of node displacements for mode i , q_i are mode amplitude coefficients, f_i is a vector of nodal forces for mode i , p_i are modal force amplitude coefficients, $[K]$ is a stiffness matrix, F is a superposition of modal forces, F_{eqm} are the forces due to any residual stress effects, $[M]$ is a mass matrix, and y is a vector of the positional state of the mesh.

However, when stress stiffening becomes significant, the modal components of the deformed structure must be determined by projecting the shape back onto the modes using the orthogonality condition:

$$\mathbf{j}_i^T [M] \mathbf{j}_j = m_i \mathbf{d}_{ij} \quad (5)$$

\mathbf{d}_{ij} is the Kronecker delta, m_i is the modal mass. Projecting back onto the modes gives us:

$$\bar{\mathbf{y}} = \bar{\mathbf{y}}_{eqm} + \sum_i^m q_i \mathbf{j}_i + \mathbf{e} = \mathbf{y}_e(q_i, \dots, q_m) \quad (6)$$

Here \mathbf{e} is the contribution of the high order modes excited by stress stiffening. It is associated with axial stretching and Poisson contraction. We note here that the shape associated with a given combination of modal amplitudes, $\mathbf{y}_e(q)$ is different from that used in the CHURN process, $\mathbf{y}_o(q)$. The former shape includes the effects of the higher order modes, which are constrained to zero amplitude in the latter. This constraint is the source of the incorrect stiffness in the CHURN model [2].

We repeat the above procedure to build up a data set. This is then fitted to a polynomial in mode amplitudes to produce the strain energy function U_m . The electrostatic co-energy must also be calculated using the new shape, $\mathbf{y}_e(q)$, in order to combine the two energies in the equation of motion. However, unlike the strain energy, we find that the electrostatic co-energy is negligibly affected by the difference, \mathbf{e} , from the original CHURN shape, $\mathbf{y}_o(q)$. Hence, we continue to employ the simpler CHURN process to generate this energy function.

In order to construct the equations of motion for the macromodel, we first calculate analytic forms for the mechanical and electrostatic forces directly from the energy functions by taking partial derivatives with respect to mode amplitudes:

$$\begin{aligned} F_{m,i}(q) &= - \frac{\partial U_m(q)}{\partial q_i} \\ F_{e,i}(q) &= + \frac{\partial U_e^*(q)}{\partial q_i} \end{aligned} \quad (7)$$

The final equations of motion (1) are now a set of m coupled ordinary differential equations, which can be inserted into system level simulators.

3 RESULTS

The data generation algorithms described in the previous section were implemented using the mechanical and electrostatic solvers provided in the MEMCAD [3] suite of tools. The polynomials were fitted to the data using

MATLAB [4], and the equations of motion were implemented in the system level simulator, SABER [5].

Our first example, shown in *Figure 3*, is a doubly supported beam, suspended above a ground electrode. Applying a voltage between the beam and ground actuates the beam. We compare three reduced-order model solutions with 3D meshed, simulations performed in MEMCAD (*Figure 4*). The CHURN process produces a macromodel that is stiffer than the real structure. The linear mechanics macromodel, in contrast, is less stiff than the real structure. Our macromodel follows the MEMCAD simulations well, and is within 5% of the MEMCAD solution at 90% of the ‘‘pull-in’’ voltage.

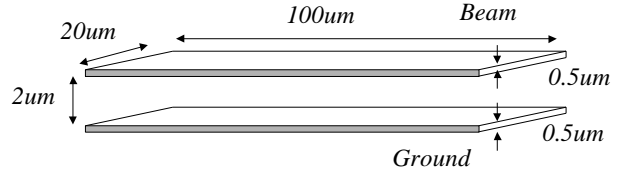


Figure 3: Diagram of a beam fixed on both ends and suspended above a ground electrode. The beam has a Young’s modulus of 165Gpa, and a Poisson’s ratio of 0.23.

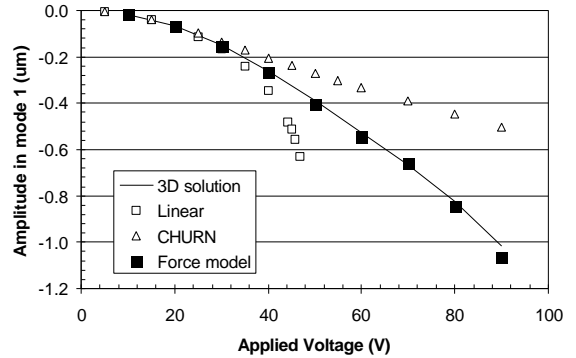


Figure 4: Graph of beam deflection vs. applied voltage. Results from a 3D, meshed, fully coupled, electromechanical simulation performed using MEMCAD’s Co-Solve simulation tool are compared to three macromodels.

The generation of the data set for this example, and other devices, involved selecting a representative set of sample points in the mode space. The CHURN process has an algorithm for selecting such a set of points. Unfortunately, this algorithm must be used with caution in the force formulation. We cannot sample a given point in mode space directly; we can only specify forces necessary to displace a structure to the required shape. Since the relationship between forces and displacement is unknown to begin with, the algorithm breaks down. Our solution is to approximate the given forces by assuming a linear system, and then adaptively improving the approximation as the data set increases in size. Currently this is done manually, however, we intend to automate the procedure.

The second example demonstrates the force method on an asymmetrically supported plate with an off-center actuation electrode. The first six elastic modes were used

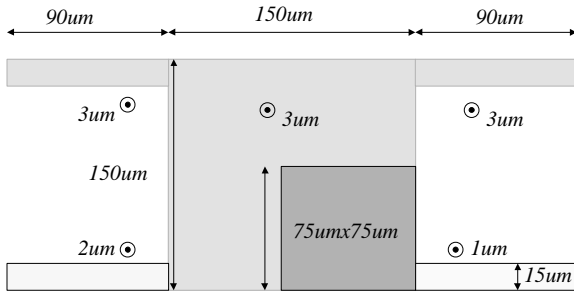


Figure 5: Asymmetrically supported plate. The actuation electrode ($75\mu\text{m}\times 75\mu\text{m}$) is located $6\mu\text{m}$ below the bottom of the plate. The plate and supports have a Young's modulus of 165Gpa , and a Poisson's ratio of 0.23 .

to model this device. 200 mechanical simulations, and 200 electrostatic simulations were performed to generate data sets for U_m and U_e . However, both functions used polynomials with approximately 90 fitting coefficients. This indicates that the number of simulations required in the data sets could significantly be reduced. The minimum number of data points that are required to accurately construct the energy functions is a topic for further investigation.

The time taken for the construction of the macromodel was approximately 10 hours on a SUN Ultra 30 workstation running at 200Mhz. Simulations performed using the macromodels in the system level simulator, SABER, took less than 10 seconds to complete.

Figure 6 is a graph of the first mode amplitude against the applied voltage. Stress-stiffening is significant at 200V and we observe the divergence of the linear model from the MEMCAD solution. The force model, however, is accurate to within 1% at 200V. Figure 7 shows the response of modes 2,3 and 4 to the applied voltage. The force model is within 5% of the MEMCAD solution at 200V.

We make a note here that the macromodel was significantly inaccurate at very small amplitudes ($<10\text{nm}$). We believe this is a result of errors in the method of projecting shapes back onto the modes during the data set construction. The current projection method cannot resolve small amplitudes in modes if one of the modes has large amplitude.

4 CONCLUSIONS

We have demonstrated a methodology for generating macro-models for stress-stiffened MEMS devices using modal basis functions. Unlike previous work, this method requires no additional user intervention than was required by the CHURN process. The models are compact and fast and can be used directly in system level simulators. Additional work is required to automate the method.

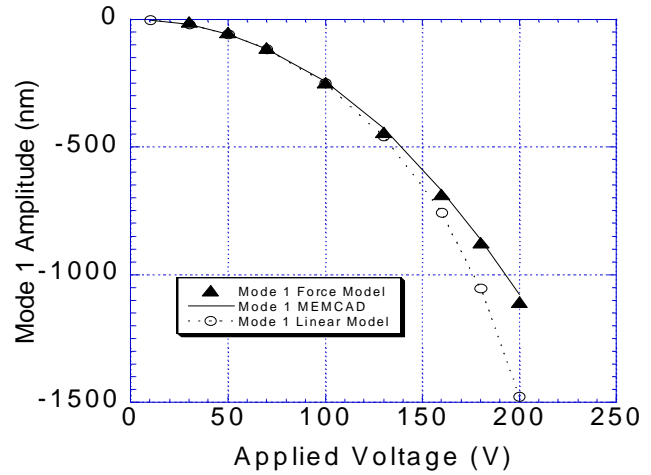


Figure 6: Mode 1 amplitude vs. applied voltage for the asymmetric plate.

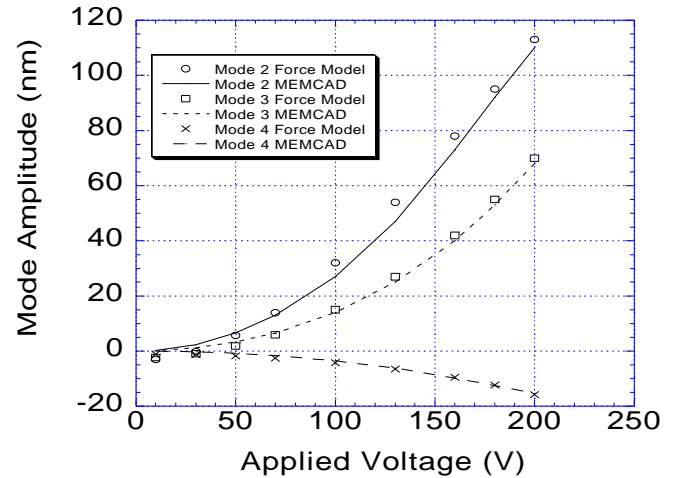


Figure 7: Mode 2,3, and 4 amplitudes vs. applied voltage for the asymmetric plate.

5 ACKNOWLEDGEMENTS

This project was sponsored by DARPA, under contract F30602-97-2-033.

REFERENCES

- [1] Lynn D. Gabbay, Jan E. Mehner, and Stephen D. Senturia, "Computer-Aided Generation of Nonlinear reduced-Order Dynamic Macromodels: I. Non-Stress-Stiffened Case," J. Microelectromechanical Systems, in press.
- [2] Jan E. Mehner, Lynn D. Gabbay, and Stephen D. Senturia, "Computer-Aided Generation of Nonlinear reduced-Order Dynamic Macromodels: II Stress-Stiffened Case," J. Microelectromechanical Systems, in press.
- [3] MEMCAD, Microcosm Technologies, Cambridge, Massachusetts, <http://www.memcad.com>
- [4] MATLAB, The MathWorks, Inc., Natick, MA 01760, <http://www.mathworks.com>
- [5] SABER, Analogy, Inc. Beaverton, OR 97008, <http://www.analogy.com>